8

Sediment Transport Modelling and Morphological Trends at a Tidal Inlet

Sandra Plecha[1], Paulo A. Silva[1],
Anabela Oliveira[2] and João M. Dias[1]
[1]*CESAM &University of Aveiro*
[2]*National Laboratory of Civil Engineering*
Portugal

1. Introduction

Currently it is of great concern the morphological changes observed at distinct coastal systems. Frequently, drastic episodes of coastal erosion, threatening the houses built near the shore, and land loss are reported. At coastal lagoons and estuaries, increasing accretion can interfere with the water renewal and therefore with the local ecosystems. At inland harbors, the accretion of inlet and channels can restrict the navigation and consequently the harbor conditions and its management.

The sediment transport, identified by patterns of erosion or accretion, can be evaluated by single formulae that compute the bedload and suspended load or by sediment transport models.

In the literature are published formulae for bed-load transport of sediments in conditions characteristic of coastal waters, covering current alone, current plus symmetrical waves, current plus asymmetrical waves alone and integrated longshore transport.

Due to the fact that sand transport models are often based on semi-empirical equilibrium transport formulae that relate sediment fluxes to physical properties, such as velocity, depth and grain size, it is crucial to perform sensitivity analysis of the formulae used.

Pinto *et al.* (2006) compared four sediment transport formulations considering only the tidal current only: Ackers and White (1973); Engelund and Hansen (1967); van Rijn (1984a,b,c) and Karim and Kennedy (1990). The authors concluded that the van Rijn formula is the most sensitive to basic physical properties. Hence, it should only be used when physical properties are known with precision.

The sediment transport modules, coupled with hydrodynamic and wave modules compose the morphodynamic models, resulting in very complex systems emergent in the last years. In the past 30 years, morphodynamic models have been developed (Nicholson *et al.*, 1997). Among them the MIKE21, developed by the Danish Hydraulic Institute - DHI (Warren and Bach, 1992) and DELFT3D, by WL|Delft Hydraulics - DH (Roelvink and Banning, 1994), are the most popular. Most of the morphodynamic studies are generally related on engineering methods and techniques for coastal defense.

The DELFT3D model was applied by several authors, such as Grunnet *et al.* (2004), Xie *et al.* (2009) and Tung *et al.* (2009), between others. Grunnet *et al.* (2004) applied DELF3D to

hindcast the morphological development of shoreface nourishment along the barrier island of Terschelling, The Netherlands. The morphodynamic results showed a dependency on the spatial scale: on the scale of the bed level evolution with respect to bar migration and growth, model predictions are poor as the nearshore bars are predicted to flatten out. On the other hand, the model satisfactory predicted the overall effects of the nourishment taking into account the mass volumes integrated over larger spatial scales.

Successful results were obtained by Xie *et al.* (2009) in the analysis of the physical processes and mechanisms essential to the formation and evolution of a tidal channel in the macro-tidal Hangzhou Bay, China. This work shows that the model results reproduced accurately the real morphological features. The results showed that spatial gradients of flood dominance, caused by boundary enhancement via current convergences, are responsible for the formation of the channel system, due to, between other effects, the funnel-shaped geometry.

DELFT3D was also applied to model inlets morphodynamics. Tung *et al.* (2009) investigate the migration and closure of an idealized tidal inlet system due to wave driven longshore sediment transport. The authors reproduced a typical example of a migrating tidal inlet due to oblique waves that include features such as ebb channel formation, migration and welding to the downdrift barrier. It was also reproduced the inlet closure due to the prolongation of the inlet channel and infilling with littoral-drift material.

Other morphodynamic modeling systems were developed and applied to coastal lagoons and inlets. For example, Ranasinghe *et al.* (1999) developed a morphodynamic model capable of simulating the seasonal closure of inlets, including both longshore and cross-shore transport processes. This model was successfully applied to two idealized scenarios demonstrating its ability to produce realistic results. Later, Ranasinghe and Pattiaratchi (2003) used field experiments and this numerical model to study a real case, the Wilson Inlet at Western Australia. With this study they identified the morphodynamic processes governing seasonal inlet closure and determined the effect of the seasonal closure of the inlet on the morphodynamic characteristics of the adjacent estuary/lagoon. These authors concluded that the inlet closure is due to the onshore sediment transport induced by persisting swell wave conditions during summer.

Cayocca (2001) developed and applied a two-dimensional horizontal morphodynamic model, combining modules for hydrodynamics, waves, sediment transport and bathymetry updates, to Arcachon lagoon, at the French coast. The results showed that the tide is responsible for the opening of a new channel at the extremity of the sand pit, while waves induce a littoral transport responsible for the longshore drift of sand bodies across the inlet.

Work *et al.* (2001) described and applied a modeling system (Mesoscale Inlet Morphology, MIM) that include coupled modules of hydrodynamic, wave transformation, shoreline change and sediment transport, to the undredged and unstabilized Price Inlet, South California. The predicted bathymetric changes were similar in sign and location to the observations, but the model tends to underpredict the magnitude of changes.

Silvio *et al.* (2010) used a long term model of planimetric and bathymetric evolution of Venice lagoon. These authors applied this model to a schematic system consisting of an inlet area and a lagoon basin and considering the interactions between tidal currents, longshore currents and sea waves. It was found that the planimetric evolution of the channel network was much faster than the bathymetric evolution of the lagoon.

One aspect that contributes to the patterns of the sediment transport in a tidal inlet is the ebb/flood dominance. The processes that contribute to determine this dominance were studied by Robins and Davies (2010) through a 2D model (TELEMAC modeling system)

applied to Dyfi estuary in Wales, UK. The authors concluded that shallow water depths lead to flood dominance in the inner estuary whilst tidal flats and deep channels cause ebb dominance in the outer estuary.

Two morphodynamic modeling systems developed in Portugal are described in the literature: MOHID and MORSYS2D.

MOHID model simulates the non-cohesive sediment-dynamics in lagoons driven by tide, waves and river flows (Malhadas *et al.*, 2009). It integrates MOHID hydrodynamic (Aires *et al.*, 2005; Neves *et al.*, 2000), sand transport modules (Silva *et al.*, 2004) and the wave model STWAVE (Smith *et al.*, 2001). This model was applied to Óbidos lagoon in order to evaluate the effect of the bathymetric changes on the hydrodynamic and residence time, suggesting strategies to avoid the lagoon's accretion and to prevent the safety of local houses at the lagoon margins. The conclusions confirmed that tidal propagation depends strongly on the bathymetric configuration.

The MORSYS2D model is composed by the hydrodynamic models ADCIRC or ELCIRC, the wave model SWAN and the sediment transport and bottom update model SAND2D (Fortunato and Oliveira, 2003, 2007; Bertin *et al.*, 2009b). The performance of MORSYS2D was assessed in the morphodynamic simulation forced both by current and waves of the Óbidos lagoon and is described in Oliveira *et al.* (2004). The morphodynamic of this lagoon and its inlet have been studied and published in several works: Fortunato and Oliveira (2006, 2007); Bertin *et al.* (2007, 2009a,b); Fortunato *et al.* (2009). In these studies the authors concluded, that the sediment grain size and the choice of the empirical sediment transport formulae affect the morphological predictions. The development of a meander and the formation of sandbars in the wave dominated inlet of Óbidos lagoon had been successfully simulated also with the recently partially parallelized MORSYS2D (Bruneau *et al.*, 2010). Besides Óbidos, other inlets morphodynamics were also studied with this model, the Ancão inlet in Ria Formosa (Bertin et al., 2009c) and the Ria de Aveiro lagoon inlet (Oliveira et al., 2007, Plecha et al., 2007,2010,2011). Other studies have been performed with this modeling system: scenario test cases of an idealized dredged sandpit (Ramos *et al.*, 2005), a dredged area evolution in southern Portugal (Rosa *et al.*, 2011), the Aljezur coastal stream morphological variability (Guerreiro *et al.*, 2010).

This work presents a sensitivity analysis of several formulations usually applied for estimating the sediment transport rates in coastal lagoons and estuaries. Morphodynamic simulations are then performed at a study case inlet, the northwest coastal lagoon inlet of Ria de Aveiro, considering the selected formulations to compute the sediment transport rates with the MORSYS2D modeling system. The numerical results are analyzed concerning the morphological changes (erosion and accretion areas) induced at that site.

2. Sediment transport

The sediment transport processes are very important in estuaries and inlets being essential to describe their morphologic changes. These processes are generally complex and are function of the hydrodynamic circulation and sediment characteristics of the bed.

When describing the sediment balance at an inlet, it has to be taken into account the longshore currents induced by the waves that approach the coast at an oblique angle and the tidal currents alone or coupled with waves. The following subsections present several formulations to compute the longshore and load sediment transport rates published in literature and used frequently by researchers.

2.1 Longshore sediment transport

The sediment transport induced by longshore currents along the coast is easily identified through coastal erosion or accretion around structures. Along the coast, considerable amounts of sediment are transported, depending on the height, period and direction of the waves. Additionally, the sediment size and the bottom slope are important parameters that determine the longshore transport.

The longshore sediment transport can be calculated by means of several longshore sediment transport formulations. Herein are presented six of them. The first one was presented by Vongvisessomjai *et al.* (1983) (Chonwattana *et al.*, 2005), and was adapted from the Coastal Engineering Manual (2002) formula. In this formulation the longshore sediment transport is proportional to the wave characteristics in deep water. The remaining five formulations are published in literature (e.g. Larangeiro and Oliveira (2003)) and are proportional to the wave characteristics in the breaker line, with different dependences in wave breaker height, wave period and incident wave breaker angle.

2.1.1 Formulation CERC

This formulation is based on the assumption that the longshore transport rate depends on the longshore component of wave energy flux in the surf zone:

$$Q_\ell = 0.064208 H_0^{5/2} F(\alpha_0) f \tag{1}$$

with

$$F(\alpha_0) = \cos\alpha^{1/4} \sin 2\alpha_0 \tag{2}$$

where H_0 is the wave height in deep water, a_0 is the wave angle in deep water and f is the wave frequency.

2.1.2 Formulation C2

Valle *et al.* (1993) proposed a formulation for the longshore transport rate given by:

$$Q_\ell = \frac{k}{16\sqrt{\gamma}(\rho_s - \rho)a'} \rho H_b^{5/2} \sin 2\alpha_b \tag{3}$$

with $k = 1.4e^{-2.5d_{50}}$, the medium particle diameter is d_{50} in mm and $a' = 1 - n$ is the breaker index, ρ_s is the sand density, ρ is the water density, g is the gravity, a_b is the wave angle at breaker point and n is the sediment porosity. The wave height in this formulation is the root mean square wave height H_{rms} given by:

$$\begin{aligned} H_{rms} &= \sqrt{8m_0} \Rightarrow \sqrt{m_0} = \frac{H_{rms}}{\sqrt{8}} \\ H_s &= 4\sqrt{m_0} \Rightarrow \sqrt{m_0} = \frac{H_s}{4} \\ \frac{H_{rms}}{\sqrt{8}} &= \frac{H_s}{4} \Leftrightarrow H_{rms} = \frac{\sqrt{8}}{4} H_s \Leftrightarrow H_{rms} = \frac{\sqrt{2}}{2} H_s \end{aligned} \tag{4}$$

where H_s is the significant wave height.

2.1.3 Formulation K&I

Komar and Inman (1970) proposed a formulation for the longshore transport rate given by:

$$I_\ell = K'(Ec_g)_b \cos\alpha_b \frac{\overline{V_\ell}}{u_m} \tag{5}$$

with

$$\overline{V_\ell} = 20.7 i (gH_b)^{1/2} \sin 2\alpha_b \tag{6}$$

And

$$u_m = \frac{\gamma}{2}(gH_b)^{1/2} \tag{7}$$

where K' is a dimensionless coefficient, E is the wave energy, c_g is the wave group velocity and i is the bottom slope. By the Coastal Engineering Manual (2002):

$$I_\ell = (\rho_s - \rho) g (1-n) Q_\ell \Leftrightarrow Q_\ell = \frac{I_\ell}{(\rho_s - \rho) g (1-n)} \tag{8}$$

Thus:

$$Q_\ell = \frac{K'(Ec_g)_b \cos\alpha_b \frac{\overline{V_\ell}}{u_m}}{(\rho_s - \rho) g (1-n)} \tag{9}$$

2.1.4 Formulation Kr88

Kraus *et al.* (1988) proposed a formulation for the longshore transport rate given by:

$$I_\ell = 2.7(R - R_c) \tag{10}$$

With $R = \overline{V_\ell} W H_b$, being W the total width of the cross section and R_c a constant. By Kraus *et al.* (1988) it is known that I_ℓ has units of N s^{-1} and the coefficient 2.7 is not adimensional. By Larangeiro *et al.* (2005):

$$Q_\ell = \frac{2.7(R - R_c)}{(\rho_s - \rho) g (1-n)} \tag{11}$$

2.1.5 Formulation K86

Kamphuis *et al.* (1986) proposed a formulation for the longshore transport rate given by:

$$Q_\ell = \frac{1.28}{(\rho_s - \rho)(1-n)} H_b^{7/2} i d_{50}^{-1} \sin 2\alpha_b \tag{12}$$

2.1.6 Formulation K91

Kamphuis (1991) proposed a formulation for the longshore transport rate given by:

$$Q_\ell = \frac{2.27}{(\rho_s - \rho)(1-n)} H_b^2 T_p^{1.5} i^{0.75} d_{50}^{-0.25} \sin^{0.6} 2\alpha_b \quad (13)$$

where the peak period is $T_p = 2.07 T_z - 4.02$ and T_z is the zero-upcrossing wave period.

2.2 Sensitivity analysis to longshore sediment transport formulations

To choose which one of the previous formulations is the most adequate to use in a study case, it is mandatory to perform a sensitivity analysis of the sediment transport formulations to several characteristics: sediment size d_{50} and bottom slope i. The analysis of the results should be performed knowing à priori a range of longshore transport values in order to compare the values obtained.

In this case, the longshore sediment transport is calculated by means of the six longshore sediment transport formulations presented in the previous subsection. Each one of this formulation has a different dependency on the wave height and angle at the breaker line and on d_{50} and bottom slope. These dependencies are presented in Table 1.

Formulation	$Q_\ell (m^3 year^{-1})$	$K \propto$
C2	$K_1 H_{rms}^{5/2} \sin 2\alpha_b$	$e^{d_{50}}$
K&I	$K_2 H_b^{5/2} \cos\alpha_b \sin 2\alpha_b$	i
Kr88	$K_3 H_b^{3/2} \sin 2\alpha_b W$	i
K86	$K_4 H_b^{7/2} \sin 2\alpha_b$	$d_{50}^{-1} i$
K91	$K_5 H_b^2 T_p^{1.5} \sin^{0.6} 2\alpha_b$	$d_{50}^{-0.25} i^{0.75}$

Table 1. Longshore sediment transport formulations.

It should be noted that all these formulae make use of significant wave height, except the C2 formulation which accounts for the root mean square wave height, H_{rms}. The K&I, Kr88, K86 and K91 formulations depend on the bottom slope and only the C2, K86 and K91 have dependencies on the sediment size d_{50}. The longshore sediment transport is computed considering a wave regime of 11 years long of the study area and typical values for the sediment size d_{50} and bottom slope, presented in bibliography or measured in situ. However, as these two parameters are not known accurately, a sensitivity analysis of the several formulations to typical values of d_{50} and i was performed. Figure 1 illustrated the results obtained for the formulations presented for typical ranges of d_{50} and bottom slope of the northwest Portuguese nearshore

It is observed that there is a wide spread of results for the longshore sediment transport. The K86 formulation revealed to be highly sensitive to the value of d_{50} considered, due to its inverse dependency on the sediment size. Also, the C2 formulation, with an exponential dependency on d_{50} revealed a strong dependency to this parameter. Analyzing the results of the dependency of longshore sediment transport to the bottom slope, again the K86 formulation shows the higher dependency due to the linear dependency on slope i. The same dependency and sensible behavior is obtained when using the K&I formulation to compute the longshore sediment transport.

The reference value for the longshore sediment transport of the Portuguese Aveiro west coast considered was presented by Larangeiro and Oliveira (2003) and is Q_ℓ =1×10^6 m^{3}year^{-1}.

Analyzing the values obtained in Figure 1, it is concluded that the longshore sediment transport computed for the complete wave regime by all transport formulae is overestimated when compared with the reference value.

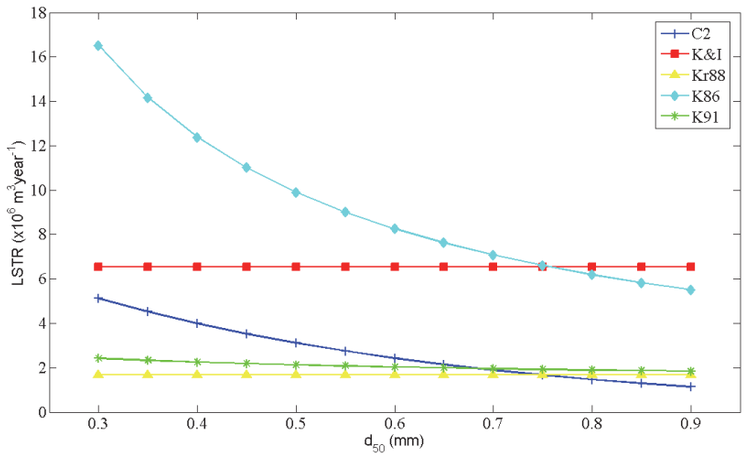

(a)

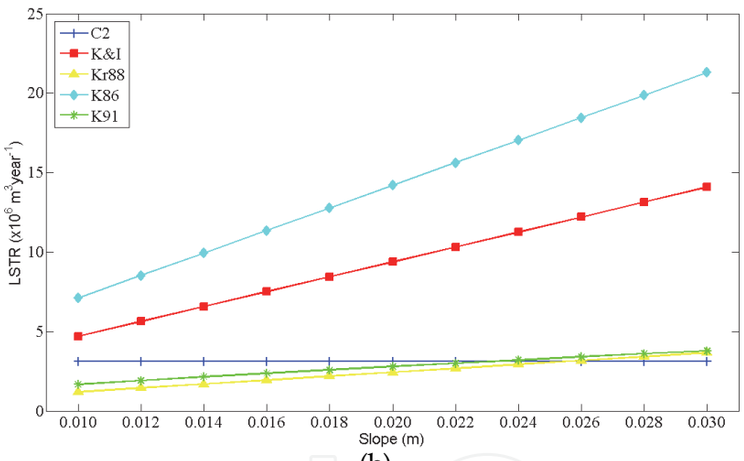

(b)

Fig. 1. Sensitivity analysis of the longshore sediment transport formulations to (a) d_{50} (mm) and (b) the bottom slope (m).

2.3 Sediment transport formulations

Usually the sediment load is subdivided into bedload and suspended load. The bedload is defined as the part of the total load that is in more or less continuous contact with the bed during the transport. It primarily includes grains that roll, slide or jump along the bed. The suspended load is the part of the total load that is moving without continuous contact with the bed as a result of the agitation of fluid turbulence (Fredsoe and Deigaard, 1992).

The nonlinear dependency of the sediment transport to the current velocity makes the net transport through inlets very sensitive to ebb/flood tidal asymmetries.

The initiation of bed sediments movement occurs when the bottom shear stress exceeds a critical shear stress defined by the gravitational force, the frictional forces on the bed and the sediment size.

The rates of sediment transport can be computed by several formulations that compute the total load considering the forcing of tidal currents or the coupled effect of tidal currents and waves. Herein are presented 8 formulations. A sensitivity analysis of these formulations is performed in subsection 2.4. These formulations integrate the morphodynamic modelling system used in this study (MORSYS2D), as presented in Section 3.

2.3.1 Formulation Bha

Bhattacharya *et al.* (2007) proposed a formulation to compute the total transport directly, for the tidal current forcing:

$$\frac{q_s}{\sqrt{(s_d - 1 g d_{50}^3)}} = \begin{cases} 0.072078 \dfrac{T^{0.893}}{d_*^{0.353}} \left(\dfrac{H}{d_{50}} \right)^{0.486} & T > 2.22 \\ 0.0000782 \dfrac{T^{0.54}}{d_*^{0.00407}} \left(\dfrac{H}{d_{50}} \right)^{1.16} & T \le 2.22 \end{cases} \tag{14}$$

where $T = (\theta' - \theta_{cr}) / \theta_{cr}$, is the transport stage parameter, θ_0 is the mobility parameter relative to grain roughness, θ_{cr} is the Shield critical shear stress, $d_* = d_{50}((s_d - 1)g / \nu^2)^{1/3}$ is the dimensionless grain size, d_{50} is the medium particle diameter and ν is the cinematic viscosity of the water.

2.3.2 Formulation EH

Engelund and Hansen (1967) proposed a formulation that computes the total load directly. The threshold for initiation of motion is not considered. The sediment flux forced by tidal currents is given by:

$$\vec{q_s} = \frac{0.05}{s^2 d_{50} C^3 \sqrt{g}} U^4 \vec{u} \tag{15}$$

where C is the Chézy coefficient given by $\sqrt{c_f / g}$, with c_f the friction coefficient and U is the modulus of the depth-averaged velocity.

2.3.3 Formulation kk

Karim and Kennedy (1990) proposed a formulation that computes the total load transport directly considering the effect of tidal currents. The sediment flux is given by:

$$\vec{q_s} = 10^{-2.821 + 3.369 \log(\nu 1) + 0.84 \log \nu 11)} \sqrt{(s-1) g d_{50}^3} \frac{\vec{u}}{U} \tag{16}$$

Where $\nu_1 = U / \sqrt{(s-1) g d_{50}}$ and $\nu_1 = (u_* - u_{*cr}) / \sqrt{(s-1) g d_{50}}$. U_* is the stress velocity and u_{*cr} is the critical stress velocity.

2.3.4 Formulation MPM

Meyer-Peter and Muller (1948) proposed a formulation based on experimental studies only valid for bed-load transport. Carmo (1995) improved this formulation in order to include the influence of bed-slope. The bed load sand flux forced by tidal currents is then given by:

$$q_s = \frac{8}{(s-1)g}\left(\frac{|\vec{\theta}| - \theta_c}{\rho_s}\right)^{1.5} \tag{17}$$

where s is the dimensionless sand density, θ_c is the critical Shields parameter and ρ_s is the sand density.

2.3.5 Formulation vR

van Rijn (1984a,b,c) proposed a formulation valid for bed load and suspended load transport.
The bottom slope is considered in the evaluation of the threshold for initiation of motion. The sediment flux forced by tidal currents is given by:

$$\vec{q_s} = \left(\frac{0.053}{U}\sqrt{g\frac{\rho_s - \rho}{\rho}}\frac{d_{50}^{2.1}}{d_*^{0.3}}T_{sp}^{2.1} + FHc_a\right)\vec{u} \tag{18}$$

where T_{sp} is a transport stage parameter $(=(u_*^2 - \tau_c/\rho)/(\tau_c/\rho))$, c_a is the reference concentration $(=0.015 d_{50} T_{sp}^{1.5}/(a d_*^{0.3}))$ where a is the reference level given by:

$$a = \begin{cases} 3d_{90} + 1.1\Delta\left(1 - \exp\left(-25\Delta/\Lambda\right)\right) & T_{sp} < 25 \\ 3d_{90} & T_{sp} \geq 25 \end{cases} \tag{19}$$

With $\Delta = 0.11H(d_{50}/H)^{0.3}(1-\exp(-T_{sp}/2))(25 - T_{sp})$ is the dune height and $\Lambda = 7.3H$ is the dune length.
A minimum value of a is set to H/100. In equation 2.21 F is given by:

$$F = \frac{\left(\frac{a}{H}\right)^Z - \left(\frac{a}{H}\right)^{1.2}}{\left(1 - \frac{a}{H}\right)^Z (1.2 - Z)} \tag{20}$$

Where $Z = \omega/(\kappa\beta u_*) + \phi$ is the suspension parameter, where κ is the von Karman constant (=0.4), $\beta = 1 - 2(\omega^2/u_*^2)$ and $\phi = 1$ if $u_* \geq 100\omega$ and $\phi = 2.5(\omega/u_*)^{0.8}(c_a/0.65)^{0.4}$ if $u_* < 100\omega$.

2.3.6 Formulation AW

The formulation presented herein is an adaptation by van de Graaff and van Overeem (1979) of the Ackers and White (1973) formulation for currents to take into account the effect of waves. The total load is given by:

$$q_{st} = U_c \frac{1}{1-\lambda} d_{35}\left[\frac{U_{cw}}{U_{*cw}}\right]^n \frac{C_{dgr}}{A^m}\left[\frac{C_d^n U_{cw}\left(\frac{U_{*cw}}{U_{cw}}\right)^n}{C_d g^{n/2}\sqrt{\left(\frac{\rho_s}{\rho} - 1\right)d_{35}}} - A\right]^m \tag{21}$$

where λ is the sediment porosity, d_{35} the particle diameter exceeded by 65% of the weight and $A = 0.23/\sqrt{d_{gr}} + 0.14$, $n = 1 - 0.2432\ln(d_{gr})$, $m = 9.66/d_{gr} + 1.34$, $C_{dgr} = \exp(2.86\ln d_{gr} - 0.4343[\ln d_{gr}]^2 - 8.128)$. In Equation 2.23, U_{cw} and U_{*cw} are the current velocity and shear velocity modified and are given by:

$$U_{cw} = U_c\sqrt{1 + 0.5\left(\xi'\frac{U_\omega}{U_c}\right)^2} \qquad U_{*cw} = U_{*c}\sqrt{1 + 0.5\left(\xi\frac{U_\omega}{U_c}\right)^2} \tag{22}$$

With

$$\xi = 18\log\left(\frac{12H}{r}\right)\sqrt{\left(\frac{f_\omega}{r}\right)} \qquad \xi' = 18\log\left(\frac{10H}{d_{35}}\right)\sqrt{\left(\frac{f'_\omega}{2g}\right)} \tag{23}$$

where r is the bed roughness and f_w and f_w' are the wave friction coefficient using r and d_{35} as bed roughness, respectively.

2.3.7 Formulation Bi

Bijker (1971) derived a formulation for bedload transport where the total load is expressed as the sum of a bedload q_{sb} term and a suspended load q_{ss} term, considering the coupled effect of tidal currents and wave regime:

$$\begin{aligned} q_{sb} &= C_b d_{50}\frac{U_c}{C}\sqrt{g}\exp\left[\frac{-0.27(\rho_s - \rho)gd_{50}}{\mu\tau_{cw}}\right] \\ q_{ss} &= 1.83q_{sb}\left[I_1\ln\left(\frac{33H}{\delta_c}\right) + I_2\right] \end{aligned} \tag{24}$$

where C_b is a wave breaking parameter (1.0 for non breaking waves and 5.0 for breaking waves with a ramp function between the two situations), C is the Chézy coefficient based on d_{50}, μ is a ripple factor (= $(C/C_{90})^{1.5}$, where C_{90} is the Chézy coefficient based on d_{90}), I_1, I_2 are integrals and τ_{cw} is the combined shear stress due to waves and currents given by:

$$\tau_{c\omega} = \tau_c\left[1 + 0.5\left(\zeta\frac{U_c}{U_\omega}\right)^2\right] \tag{25}$$

where τ_c is the bed shear stress due to currents only, U_w the wave orbital velocity, $\zeta = C\sqrt{f_\omega/(2g)}$ is a parameter for wave-current interaction, f_w a wave friction factor and U_c is the current velocity.

2.3.8 Formulation SvR

The formulation of Soulsby and van Rijn (Soulsby, 1997) compute sediment transport under the combined action of wave and currents. The total load is given by:

$$q_{st} = A_s U_c\left[\sqrt{U_c^2 + \frac{0.018}{c_d}U_{\omega rms}} - U_{cr}\right]^{2.4}(1 - 1.6\tan\beta) \tag{26}$$

where U_{wrms} is the root mean square wave orbital velocity and β is the local bottom slope, C_d is a drag coefficient and U_{cr} is the threshold velocity. $A_s = A_{sb} + A_{ss}$ with A_{sb} and A_{ss} the terms for bedload and suspended load, respectively, given by:

$$A_{sb} = \frac{0.005H\left(\frac{d_{50}}{H}\right)^{1.2}}{\left(\left(\frac{\rho_s}{\rho}-1\right)gd_{50}\right)^{1.2}} \qquad A_{ss} = \frac{0.012d_{50}d_*^{-0.6}}{\left(\left(\frac{\rho_s}{\rho}-1\right)gd_{50}\right)^{1.2}} \tag{27}$$

where C_d is the drag coefficient $(=(0.40/(\ln(H/z_0)-1))^2)$, where z_0 is the bed roughness length. In Equation 2.28, U_{cr} is the threshold current velocity equal to $0.19d_{50}^{0.1}\log(4H/d_{90})$ if 0.1 mm ≤ d_{50} < 0.5 mm and to $8.5d_{50}^{0.6}\log(4H/d_{90})$ if 0.5 mm ≤ d50 ≤ 2.0 mm.

2.4 Sensitivity analysis of the sediment transport formulations

A sensitivity analysis of the sediment transport rates (q_s), computed from the aforementioned formulae, to the median sediment grain size d_{50}, the water depth h, and depth-averaged velocity U, is performed to better understand the response of the numerical solutions concerning bathymetric changes. These computations are made using a single point formulation that was retrieved from the numerical module of MORSYS2D that computes the sediment transport (Silva *et al.*, 2009) and considering values for d_{50}, h and U characteristics of inlets.

In Figure 2(a) is illustrated the transport rate q_s as a function of the medium sediment grain size, d_{50}, for a constant water depth of 2, 10 and 20 m and considering a steady current with a depth-averaged velocity value of 1.0, 1.5 and 2.0 ms^{-1}. In Figure 2(b) the added effect of a single wave with significant height of 1 m and 7 s of wave period was considered.

The SvR, EH, kk, vR and AW formulations show a decrease of the transport rate with increasing d_{50}, either in presence of tidal currents only (Figure 2(a)) or coupled with a monochromatic wave (Figure2(b)). Therefore, the dependency of these formulae in d_{50} is very similar. It can be noted that this dependency is non-linear; the range of variation of q_s for the fine and medium grain sizes is higher than for the coarser sand.

In Figure 2(a) is visible that the formulation by Bha predicts higher transport rates, except for the higher velocities (U = 2 ms^{-1}) or lower depths, where the results are close to those obtained with the other formulations.

The MPM formulation predicts systematically lower values of q_s, and changes with d_{50} are not very significant. Note that this formulation only takes into account the bed load transport.

The transport rates computed from Bi (in Figure 2(a) and (b)) and vR formulations present some oscillations with d_{50} that are not observed with any other formulae, in particular, for the finer sediments. When compared to formulae SvR, EH, kk and AW, the vR formula over-predicts the transport rates for finer sediments. The results predicted by all the formulations and from the ensemble of tests considered show a larger spread for the lowest values of U and finer sand than for the highest velocities and coarser sand, respectively. These results stand equally valid for the large range of depth-average tidal flow velocities observed within the inlet.

As an example, Figure 3 represents the computed net transport rates for a tidal cycle (for a neap and spring tide periods) for a local mean depth of 10 m and 20 m. The depth-averaged velocity intensity considered is illustrated in the upper panel of Figure 3, characteristic of this inlet. The transport rates were computed considering two values for the d_{50}: 0.3 and 1.5 mm.

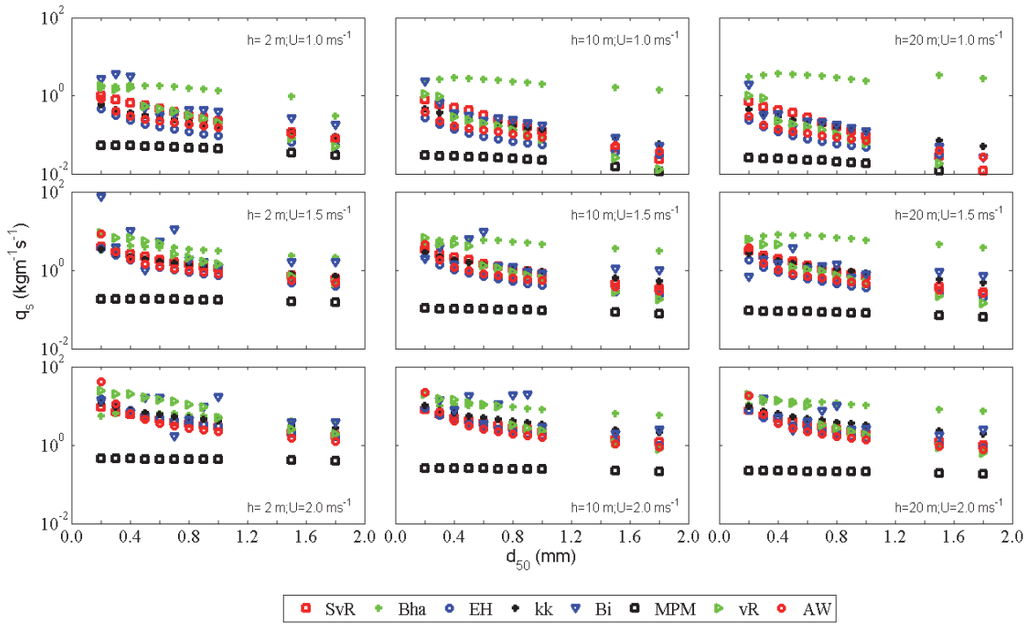

(a)

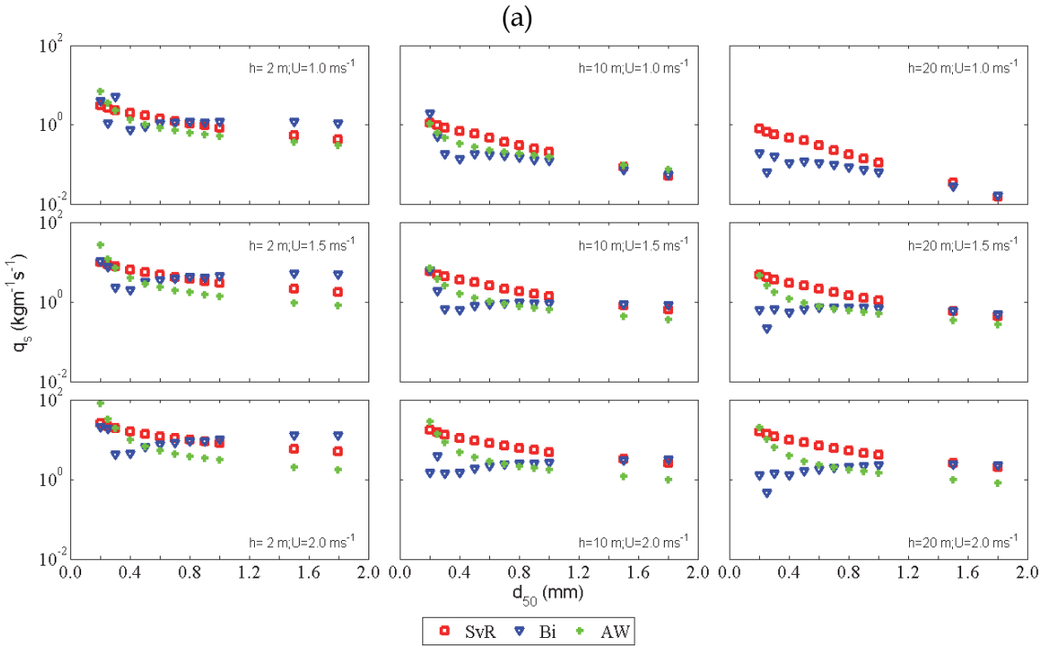

(b)

Fig. 2. Computed transport rate q_s (kgm^{-1}s) in function of d_{50} (mm), considering (a) only the tidal currents and (b) tidal currents coupled to a wave.

For any sediment grain size and any sediment transport formulation, the maximum values of q_s increase as the maximum depth-average velocities increase from neap to spring tides, and for small velocities, the transport is null. An exception to this behavior is with EH formulation, because it does not include a threshold velocity for sediment motion. Also, the sediment transport rates computed from the Bi and vR formulations present some perturbations for the highest velocities.

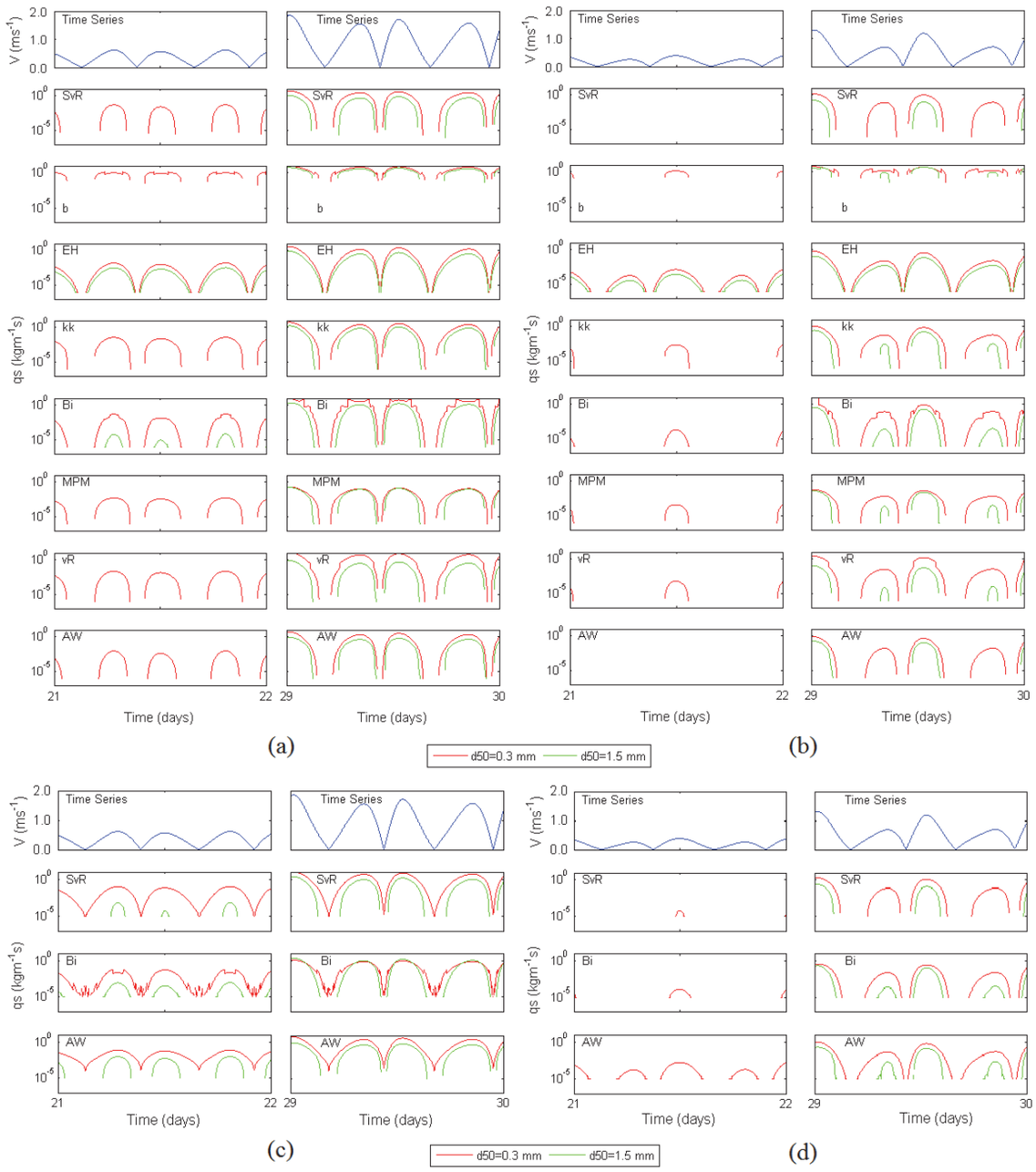

Fig. 3. Computed transport rate q_s (kgm^{-1}s) in function of d_{50} (millimetre) for velocity tidal flow computed by a hydrodynamic model forced by tidal currents only (a) and (b) and forced by tidal currents coupled with a wave regime (c) and (d), for a depth of (a) and (c) 10 m and (b) and (d) 20 m. The left (right) columns in (a), (b), (c) and (d) represent the transport rates at neap (spring) tide condition.

Analyzing Figure 2(b) it is possible to perceive that the presence of a monochromatic wave induce continuous sediment transport for lower depths (10 m in this example). For this water depth, the generated currents have the capacity to move coarser sediments, even in neap tide conditions. For Bi formulation, are observed higher instabilities in the sediment transport rates.

For the deeper water case, the effect of the wave is not strongly noticeable. However, for neap tide condition exists a slightly increasing in the capacity of transporting finer sediments.

3. Morphodynamic simulations

To the study presented herein, the morphodynamic modelling system used is the MORSYS2D (Fortunato and Oliveira, 2004, 2007; Bertin *et al.*, 2009c). This modelling system integrates the hydrodynamic model ELCIRC (Zhang *et al.*, 2004), which calculates tidal elevations and currents, the wave model SWAN (Booij *et al.*, 1999), which computes wave propagation and the model SAND2D (Fortunato and Oliveira, 2004, 2007; Bertin *et al.*, 2009c) that computes sand transports and updates the bottom topography.
This model was applied to an inlet and adjacent nearshore of a coastal lagoon in the northwest of the Iberian Peninsula, the Ria de Aveiro.
Due to the different response of the several sediment transport formulations on the sediment size and water depth as presented in the previous section, it is important to analyze the morphodynamicof the study area itself, with d_{50}, depths and currents variable in space and time.

3.1 Dependency on sediment transport formulation

In order to compare the numerical predictions using all the sediment transport formulations mentioned in Subsection 2.3, numerical simulations for a period of 1 year were performed, considering a variable d_{50} distribution, a tidal current and a wave regime variable in time. In this work a comparison of the residual sediment fluxes obtained by averaging the sand fluxes for two MSf constituent periods (2×14.78 days) was performed.
For the simulations forced only by tidal currents, the SvR, EH, kk and AW formulations predict similar patterns, contrary to the obtained with Bha (Figure 4(a)), vR (Figure 4(b)) and MPM (Figure 4(c)). The residual sediment fluxes obtained with Bha formulation, Figure 4(a), differ substantially from the other numerical solutions, predicting strong residual sediment fluxes that will induce over-prediction of the bathymetric variations and an unrealistic bathymetry. This over-prediction is consistent with previous studies presented by Fortunato *et al.* (2009) and Silva *et al.* (2009) and with that obtained in Figure 2(a).
For the vR and Bi formulations are expected oscillations in the sediment fluxes due to the patterns illustrated in Figure 3 for finer sediments and intermediate tidal velocities. In Figure 4(b) are illustrated the residual sediment fluxes computed with vR formulation, where are visible the oscillations that induce instabilities in the bathymetric predictions. On the other hand, when considering the Bi formulation, the oscillations are not easily noticeable in the residual sediment fluxes (not presented here). However, due to its sensitivity to sediment size d_{50}, this formulation should be used carefully and only when physical properties are known with precision.
In contrast to the previous results, the solutions obtained with MPM formulation (Figure 4(c)) under-predict the sediment fluxes and consequently will under-predict the bathymetric changes. This under-prediction is consistent with that obtained in Figure 3.
The numerical results obtained with the other four formulations are similar between them (SvR, EH, kk and AW (Figure 4(d))) and more realistic. The sediment fluxes at the inlet and offshore area, at the center of the navigation channel and at the beginning of the bifurcation channel, are all outward, denoting ebb dominance. Also, the residual sediment fluxes

pattern observed identifies four regions with higher values: at the inlet and offshore area, at the center of the navigation channel and at the beginning of the channels at the right side of the domain. The two first patterns referred are located in areas of strong bathymetric changes. The first one, which present the more intense flux obtained, is located in the transition from the deepest zone located between the breakwaters to shallow zones offshore. At the centre of the navigation channel, it is also observed an intense residual sediment flux, although with low intensity when compared to the former. Once again, the transition from deeper to shallower bottom originates convergence and consequently an intensification of the residual sediment flux.

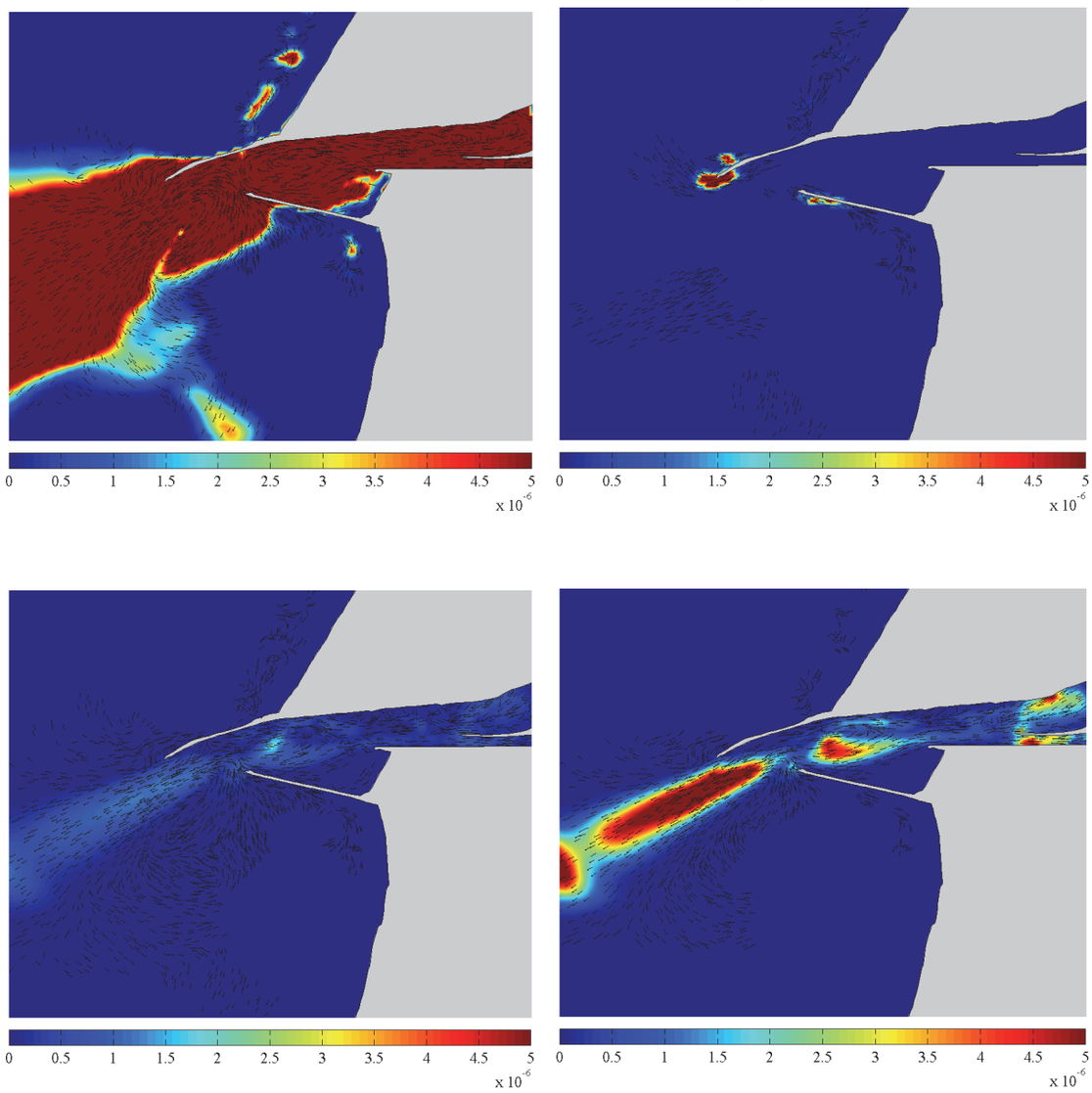

Fig. 4. Residual sediment fluxes (m^2s^{-1}) induced by tidal currents for a coastal lagoon inlet and adjacent nearshore, computed with (a) bha, (b) vR, (b) MPM and (d) AW formulations.

For the simulations forced by tidal currents coupled to a wave regime, the formulations predict similar patterns. Despite this, and for the reason pointed earlier for the case when only tidal currents forcing was considered, the Bi formulation should be used with care. The SvR formulation predicts higher residual fluxes intensities. The more realistic results were obtained with AW formulation, for the case of coupled forcing of tidal currents and wave regime. The residual sediment fluxes obtained for the AW formulation are illustrated in Figure 5.

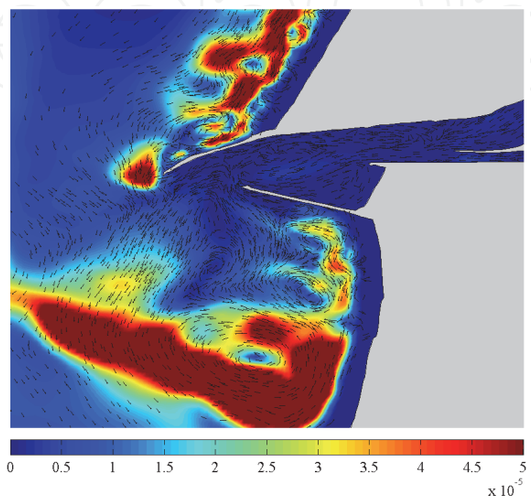

Fig. 5. Residual sediment fluxes (m^2s^{-1}) due to the forcing of tidal currents coupled with a wave regime, for a coastal lagoon inlet and adjacent nearshore, computed with the AW formulation.

When compared with the results obtained only for the tidal current forcing, it is observed that a wave regime induces one order magnitude higher sediment transport rates. In the inner areas of the inlet (inside the lagoon), the sediment transport is ruled by the tidal currents. However, at the adjacent nearshore area only the presence of a wave regime induce transport rates.

Contrasting to the general overall outward fluxes, an inward flux is observed near the south breakwater. This inward flux is induced by the currents observed at downdrift side of several inlets, where breaking waves are turned toward the inlet due to refraction over the outer bar and on breaking, creating currents toward the inlet.

At the nearshore areas higher residual transport rates are observed, predominantly directed north-south. This flux is induced by the longshore currents generated by the wave regime characteristics of the study area. At the inlet the fluxes are dominated by the outward residual tidal currents.

Comparing Figures 4 and 5, is visible that the residual fluxes patterns inside the lagoon and at the inlet are similar. In order to investigate the origin of these patterns, the influence of the sediment size d_{50} and the water depth on the residual sediment patterns is analyzed.

3.2 Dependency on d_{50} and depth

As concluded in Section 2.4, the sediment size d_{50} and the water depth have influence on the sediment transport rates. Therefore, these parameters will also have influence on the residual sediment fluxes and consequently on the bathymetric changes that occurs in the study domain.

To analyze the influence of d_{50} and the water depth on the domain morphology, numerical simulations were performed considering: a constant sediment size distribution (d_{50}); a constant depth at the study area; and the two cases coupled. All cases considered only the tidal currents forcing. Only the results obtained using the AW formulation to compute the sediment transport are presented herein.

In Figures 6 and 7 the residual sediment fluxes are illustrated considering a constant d_{50} distribution (Figure 6) and considering both d_{50} distribution (=0.5 mm) and depth (=10 m) constants (Figure 7). The results obtained considering constant depth and a heterogeneous sediment size distribution are similar to those represented in Figure 7 and are not shown.

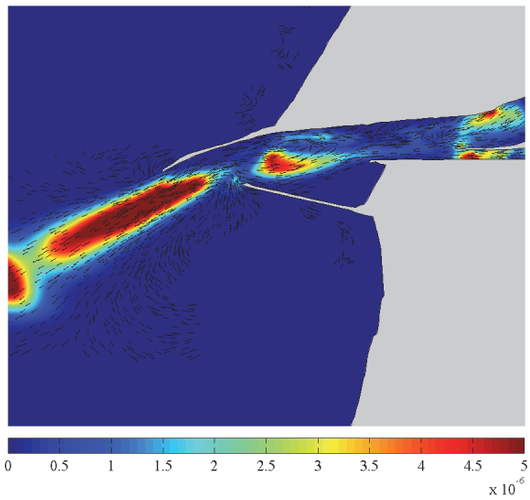

Fig. 6. Residual sediment fluxes (m^2s^{-1}) due to the forcing of tidal currents coupled with a wave regime, for a coastal lagoon inlet and adjacent nearshore, computed with the AW formulation, considering a constant d_{50} distribution.

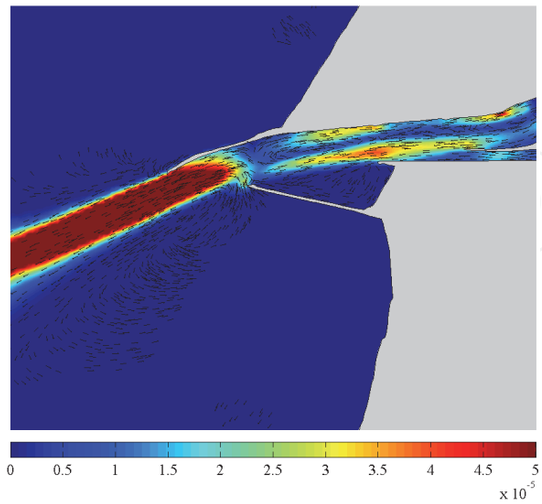

Fig. 7. Residual sediment fluxes (m^2s^{-1}) due to the forcing of tidal currents coupled with a wave regime, for a coastal lagoon inlet and adjacent nearshore, computed with the AW formulation, considering constant d_{50} distribution and constant water depth.

Analyzing Figure 6 it is observed that the residual sediment flux is very similar to that obtained when using a heterogeneous d_{50} distribution (Figure 4(d)). Thus the sediment size distribution, in this study area, is not mandatory on the definition of the residual fluxes pattern.

The results of considering a constant d_{50} distribution coupled with a constant depth set to 10 m, are illustrated in Figure 7. It is observed that the overall pattern of the residual sediment fluxes is similar to the one presented in Figure 4(d). Thus, it can be concluded that for this study area, the residual sediment fluxes are mostly originated by the geometry configuration, depending also, in minor scale, on the bathymetry.

For the study area presented herein, the geometry of the navigation channel and the configuration of the breakwaters that delimit the artificial inlet induces strong residual sediment fluxes near the north breakwater. Large bathymetric changes can result from these patterns, compromising the stability of that structure.

3.3 Trends of erosion and accretion

The residual sediment flux at a domain generates erosion or accretion locally, depending on the pattern and intensity of the flux. From the analysis of these patterns it is possible to have an idea of the bottom morphologic changes expected. In areas where the residual fluxes converge with large intensity, erosion patterns are observed due to the high amount of sediments that are transported.

As example, in Figure 8(a), (b) and (c) are illustrated the final bathymetry and the bathymetric changes induced by the residual sediment flux illustrated in Figure 5, for a one year period simulation. The white areas in figure illustrating the difference between the final and initial bathymetry represent unchanged depth, and the solid lines represent the initial bathymetry.

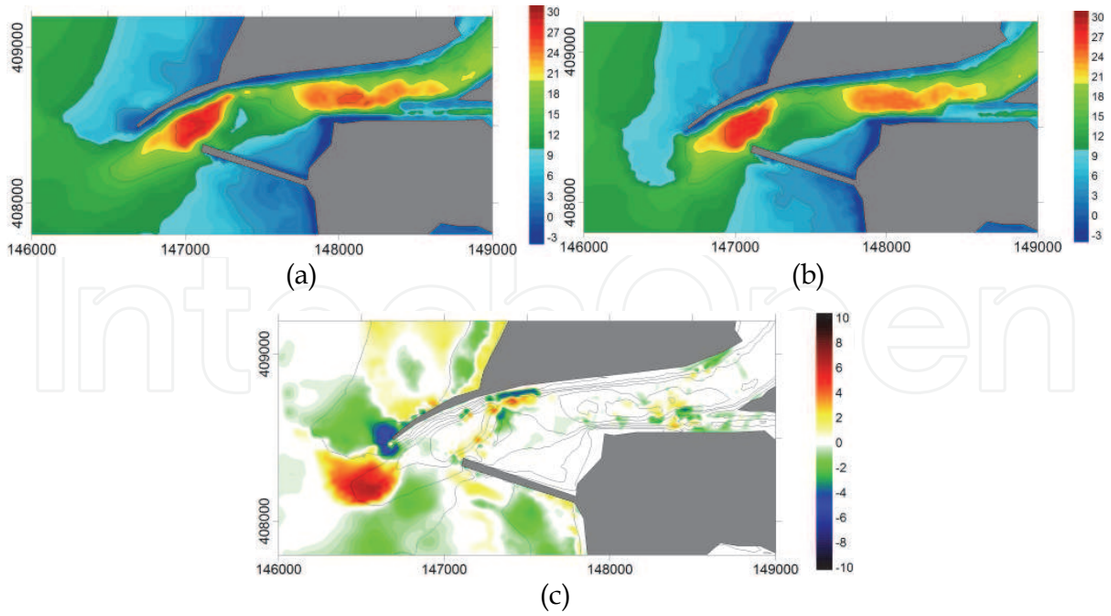

Fig. 8. (a) Initial and (b) final bathymetries (metre) for numerical simulations and (c) difference between the initial and computed final bathymetry (metre). In (c) the solid lines illustrate the initial bathymetry. The negative (positive) values represent erosion (accretion). The values in axes are in metres.

The residual sediment flux patterns at the inlet generates an erosion trend at the downstream side of the deeper zone located between the heads of the breakwaters. At the upstream side of this bottom feature and due to the decrease in the residual sediment flux, an accretion trend is obtained. The high magnitude of the residual sediment flux at the beginning of the channels at the right side of the domain (near the side walls) induces erosion trends. At the downstream side of the bifurcation, the orientation and decrease of the fluxes generates accretion trends.

4. Conclusion

There are several formulations published in literature used to compute the sediment transport rates, either as longshore or as bedload and suspended load. These formulations have different dependencies on lagoon characteristics such as sediment size d_{50}, bottom slope, water depth, current velocities and wave characteristics.

A sensitivity analysis to longshore formulations revealed that the K86 formulation is highly sensitive to the value of d_{50} and bottom slope considered, due to its inverse dependency on the sediment size and linear dependency on the bottom slope i. Also, the C2 formulation, with an exponential dependency on d_{50} revealed a strong dependency to this characteristic. The K&I formulation revealed sensible behavior to the value defined to the bottom slope.

The results obtained with the formulations of Bhattacharya *et al.* (2007) and Bijker (1967) over-predict the observed bathymetric changes, while the formulation of Msoeyer-Peter and Muller (1948) under-predicts the bathymetric variations. The results obtained with the formulations of Engelund and Hansen (1967), Ackers and White (1973), Karim and Kennedy (1990), van Rijn (1984a, b, c) and Soulsby–van Rijn (Soulsby 1997) seem to result in predictions more consistent. These conclusions are also illustrated by the spatial distribution of the residual sediment fluxes in a tidal inlet.

The analysis of sensibility performed also illustrates that the dependence of the sediment transport on d_{50} is more important for the fine–medium sediments. It was also concluded that the distribution of the sediment size is not influent on the residual sediment flux patterns. The major influence comes from the geometry of the inlet channel and also, in minor magnitude, from the bathymetric configuration.

Concerning the Ria de Aveiro inlet study area, the sediment fluxes obtained for simulations forced only by tidal currents are restricted to the navigation channel, dominating the long term transport in this zone. At the inlet the fluxes are still dominated by the seaward tidal currents, however near the north side of the inlet, they are affected by the longshore currents. At the inner sections of the lagoon mouth the fluxes induced by the tidal currents are higher than those produced only by the wave regime. At the nearshore area the sediment fluxes are only due to the influence of the wave regime. Therefore, an accurate estimation of the longshore sediment transport should be performed to describe the morphodynamics of this coastal area.

The analysis of the residual sediment transport allows the prediction of the erosion and accretion trends: in areas where the residual fluxes converge with high intensity, erosion patterns are observed due to the high amount of sediments that are transported.

Although these results were obtained for the specific case of Ria de Aveiro inlet, they can be extrapolated to understand and predict other similar systems.

5. Acknowledgement

The first author of this work is supported by the FCT through a PhD grant (FRH/BD/29368/2006). This work has been partly supported by FCT and by European Union (COMPETE, QREN, FEDER) in the frame of the research projects: POCI/ECM/59958/2004: EMERA – Study of the Morphodynamics of the *Ria de Aveiro* Lagoon Inlet; GRID/GRI/81733/2006: G-cast – Application of GRID-computing in a coastal morphodynamics nowcast-forecast system and PTDC/AAC-CLI/100953/2008: ADAPTARia – Climate Change Modelling on Ria de Aveiro Littoral - Adaptation Strategy for Coastal and Fluvial Flooding. The authors would like to thank Profs. A.M. Baptista and Joseph Zhang for the model ELCIRC (www.stccmop.org/CORIE/modeling /elcirc/index.html), the Aveiro Harbor Administration for providing the bathymetric data and the people involved in the EMERA project, in particular, Maria Virgínia Martins, for the sediment characteristics. The authors would like also to thank to André Fortunato, Xavier Bertin and Nicolas Bruneau, from LNEC, for the help provided in the implementation of MORSYS2D to the *Ria de Aveiro*.

6. References

Ackers, P. & White, W.R. (1973). Sediment transport: a new approach and analysis. *J Hydraul Div*, Vol.99, pp. 2041–2060

Aires, J.P.; Nogueira, J. & Martins, H. (2005). Survival of sardine larvae o_ the Atlantic Portuguese coast: a preliminary numerical study. *ICES Journal of Marine Science*, Vol.62, pp. 634-644

Bertin, X.; Fortunato, A.B. & Oliveira, A. (2007). Sensitivity analysis of a morphodynamic modeling system applied to a Portuguese tidal inlet. In: *5th IAHR Symposium on River, Coastal and Estuarine Morphodynamics*, Netherlands

Bertin, X.; Fortunato, A.B. & Oliveira, A. (2009a) A modeling-based analysis of processes driving wave-dominated inlets. *Cont Shelf Res*, Vol.29, No.5–6, pp. 819–834

Bertin, X.; Fortunato, A.B. & Oliveira, A. (2009b). Simulating morphodynamics with unstructured grids: description and validation of a modeling system for coastal applications. *Ocean Model,* Vol.28, No.1–3, pp. 75–87

Bertin, X.; Fortunato, A.B. & Oliveira, A. (2009c). Morphodynamic modeling of the Ancão inlet, South Portugal. *Journal of Coastal Research*, Vol.SI56, pp. 10-14

Bhattacharya, B.; Price, R.K. & Solomatine, D.P. (2007). A machine learning approach to modeling sediment transport. ASCE *J Hydraul Eng*, Vol.133, No.4, pp. 440–450

Bijker, E.W. (1971). Longshore transport computations. *J Waterway, Ports, Harbor, Coastal and Ocean Eng,* Vol.97, No.4, pp. 687-703

Booij, N.; Ris, R. & Holthuijsen, L. (1999). A third-generation wave model for coastal regions. 1. Model description and validation. *Journal of Geophysical Research,* Vol.104, No.7, pp. 649-666

Bruneau, N.; Fortunato, A.B.; Oliveira, A.; Bertin, X.; Costa, M. & Dodet, G. (2010). Towards long-term simulations of tidal inlets: performance analysis and application of a partially parallelized morphodynamic modeling system. In: *XVIII International Conference on Water Resources*. Spain

Carmo, J.S.A. (1995). Contribuição para o Estudo dos Processos Morfodinâmicos em Regiões Costeiras e Estuarinas. PhD dissertation, University of Coimbra, Portugal, pp.238

Cayocca, F. (2001). Long-term morphological modeling of a tidal inlet: the Arcachon Basin, France. *Coastal Engineering*, Vol.42, pp. 115-142

Chonwattana, S.; Weesakul, S. & Vongvisessomjai, S. (2005). 3D Modeling of morphological changes using representative waves. *Coastal Engineering Journal*, Vol.47, No.4, pp. 205-229

Coastal Engineering Manual (2002) US Army Corps of Engineers

Engelund, F. & Hansen, F. (1967). *A Monograph of Sediment Transport in Alluvial Channels.* Teknisk Forlag, Copenhagen

Fortunato, A.B. & Oliveira, A. (2004). A modeling system for long-term morphodynamics. *J Hydraul Res*, Vol.42, No.4, pp. 426–434

Fortunato, A.B. & Oliveira, A. (2006). Uma comparação de métodos para melhorar a stabilidade de um sistema de modelos morfodinâmico. In: *Conferência Nacional de Métodos Numéricos em Mecânica dos Fluidos e Termodinâmica*, Portugal

Fortunato, A.B. & Oliveira, A. (2007). Improving the stability of a morphodynamic modeling system. *J Coastal Res*, Vol.SI50, pp. 486–490

Fortunato, A.B.; Bertin, X. & Oliveira, A. (2009). Space and time variability of uncertainty in morphodynamic simulations. *Coastal Engineering,* Vol.56, pp. 886-894

Fredsoe, J. & Deigaard, R. (1992). *Mechanics of Coastal Sediment Transport,* World Scientific Publishing Co., ISBN 9810208405, Singapore

Grunnet, N.M.; Walstra, D.-J. R. & Ruessink, B. G. (2004). Process-based modelling of a shoreface nourishment. *Coastal Engineering*, Vol.51, pp. 581-607

Guerreiro, M.; Fortunato, A.B.; Oliveira, A.; Bertin, X.; Bruneau, N. & Rodrigues, M. (2010). Simulation of morphodynamic processes in small coastal systems: application to the Aljezur coastal stream (Portugal). In: *Geophysical Research Abstracts*. Vol.12

Kamphuis, J.W. (1991). Alongshore sediment transport rate. *J Waterway Port Coastal and Ocean Eng*, Vol.117, No.6, pp. 624-641

Kamphuis, J. W.; Davies, M. H.; Nairn, R. B. & Sayao, O. J. (1986). Calculation of littoral sand transport rate. *Coastal Engineering,* Vol.10, No.1, pp. 1-21

Karim, M.F. & Kennedy, J.F. (1990). Menu of coupled velocity and sediment discharge relation for rivers. *J Hydraul Eng*, Vol.116, No.8, pp. 978–996

Komar, P.D. & Inman, D.L. (1970). Longshore sand transport on beaches. *Journal of Geophysical Research*, Vol.75, No.30, pp. 5514-5527

Kraus, N.C.; Gingerich, K.J. & Rosati, J.D. (1988). Towards an improved empirical formula for longshore sand transport. In: *Proceedings of the 21st International Conference on Coastal Engineering*, New York, pp. 1183-1196

Larangeiro, S.H.C.D. & Oliveira, F.S.B.F. (2003). Assessment of the longshore sediment transport at Buarcos beach (West coast of Portugal) through different formulations. In: *CoastGis'03,* Genova

Meyer-Peter, E. & Muller, R. (1948). Formulas for bed-load transport. Proc. *3rd Meeting IAHR*, Stockholm, pp. 39–64

Malhadas, M.S.; Silva, A.; Leitão, P.C. & Neves, R. (2009). Effect of the bathymetric changes on the hydrodynamic and residence time in Óbidos lagoon (Portugal). *Journal of Coastal Research,* SI56, pp. 549-553

Neves, R.J.J.; Leitão; P.C.; Braunschweig, F.; Martins, F.; Coelho, H.; Santos, A. & Miranda, R. (2000). The advantage of a generic coordinate approach for ocean modeling. In: *Proceedings of Hydrosoft 2000 Conference,* Lisbon, Portugal.

Nicholson, J.; Broker, I.; Roelvink, J.A.; Price, D.; Tanguy, J. M. & Moreno, L. (1997). Intercomparison of coastal area morphodynamic models. *Coastal Engineering*, Vol.31, No.1, pp. 97-123

Pinto, L.; Fortunato, A.B. & Freire, P. (2006). Sensitivity analysis of non-cohesive sediment transport formulae. *Continental Shelf Research*, Vol.26, pp. 1826-1829

Oliveira, A.; Fortunato, A.B. & Sancho, F.E.P. (2004). Morphodynamic modeling of the Óbidos lagoon. *Coastal Engineering,* Vol.3, pp. 2506-2518

Oliveira, A.; Fortunato, A.B. & Dias, J.M. (2007). Numerical modeling of the Aveiro inlet dynamics. In: *Proceedings of the 30th International Conference on Coastal Engineering*. Vol.4, pp. 3282-3294

Plecha, S.; Rodrigues, S.; Silva, P.; Dias, J.M.; Oliveira, A. & Fortunato, A.B. (2007). Trends of bathymetric variations at a tidal inlet. In: Dohmen-Janssen M, Hulscher S (eds) Proceedings of the *5th IAHR Symposium on River, Coastal and Estuarine Morphodynamics*. Enschede, The Netherlands, pp. 19–23. ISBN: 0415453631

Plecha, S.; Silva, P.A.; Vaz, N.; Bertin, X.; Oliveira, A.; Fortunato, A.B. & Dias,J.M. (2010). Sensitivity analysis of a morphodynamic modeling system appliedto a coastal lagoon inlet. *Ocean Dynamics*, Vol.60, pp. 275-284

Plecha, S.; Silva, P.A.; Oliveira, A. & Dias, J.M. (2011). Establishing the Wave Climate Influence on the Morphodynamics of a Coastal Lagoon Inlet. *Ocean Dynamics*, submitted

Plecha, S.; Rodrigues, S.; Silva, P.; Dias, J.M.; Oliveira, A. & Fortunato, A.B. (2007). Trends of bathymetric variations at a tidal inlet. In: Dohmen-Janssen M, Hulscher S (eds) Proceedings of the *5th IAHR Symposium on River, Coastal and Estuarine Morphodynamics*. Enschede, The Netherlands, pp. 19–23. ISBN: 0415453631

Ramos, M.; Silva, P.A. & Sancho, F. (2005). *Morphological Modelling Using a 2DH Model. SANDPIT - Sand Transport and Morphology of Offshore Sand Mining Pits*. Aqua Publications. The Netherlands

Ranasinghe, R. & Pattiaratchi, C. (2003). The seasonal closure of tidal inlets: causes and effcts. *Coastal Engineering Journal*, Vol.45, No.4, pp. 601-627

Ranasinghe, R.; Pattiaratchi, C. & Masselink, G. (1999). A morphodynamic model todmulate the seasonal closure of tidal inlets. *Coastal Engineering*, Vol. 37, pp. 1-36

Robins, P.E. & Davies, A.G. (2010). Morphological controls in sandy estuaries: the inuence of tidal ats and bathymetry on sediment transport. *Ocean Dynamics*, Vol.60, pp. 503-517

Roelvink, J.A. & Banning, G.K.F.M. (1994). Design and development of Delf3D and application to coastal morphodynamics. *Hydroinformatics*, Vol.94, pp. 451-455

Rosa, J.; Gonçalves, D.; Silva, P.A.; Pinheiro, L.M.; Rebêlo, L.; Fortunato, A.B. & Bertin, X. (2011). Estudo da evolução de uma área de extracção de sedimentos ao largo de Vale de Lobo (Algarve – Portugal) – Comparação entre resultados numéricos e dados batimétricos adquiridos. *Revista de Gestão Costeira Integrada* (submitted)

Silva, A.J.R.; Leitão, J.C. & Abecassis, C. (2004). Improving the navigability and safety conditions in Douro estuary inlet. In: ASCE (Ed.), *Proceedings of International Conference in Coastal Engineering 2004*, pp. 3277-3289

Silva, P.; Bertin, X.; Fortunato, A.B. & Oliveira, A. (2009). Intercomparison of sediment transport computations in current and combined wavecurrent conditions. *J Coastal Res*, SI56, pp. 559–563

Silvio, G.D.; Dall'Angelo, C.; Bonaldo, D. & Fasolato, G. (2010). Long-term model of planimetric and bathymetric evolution of a tidal lagoon. *Continental Shelf Research,* Vol.30, pp. 894-903

Smith, J. M.; Sherlock, A. R. & Resio, D. T. (2001). *Steady-state Wave Model User's Manual for STWAVE. V3.0*. U.S Army Engineer Research and Development Center, Vicksburg

Soulsby, R. (1997). *Dynamics of Marine Sands.* Thomas Telford Publications, London

Tung, T. T.; Walstra, D.-J. R.; van de Graaff, J. & Stive, M. J. (2009). Morphological modeling of tidal inlet migration and closure. *Journal of Coastal Research*, SI56, pp. 1080-1084

Valle, R.; Medina, R. & Losada, M.A. (1993). Dependence of coefficient K on grain size. *J Waterways, Port, Coastal and Ocean Eng*, Vol.119, No.5, pp. 568-574

van de Graaff, J. & van Overeem, J. (1979). Evaluation of sediment transport formulae in coastal engineering practice. *Coastal Engineering,* Vol.3, pp. 1-32

van Rijn, L.C. (1984a). Sediment transport—part 1: bed load transport. *J Hydraul Eng* Vol.110, No.10, pp. 1431–1456

van Rijn, L.C. (1984b). Sediment transport–part 2: suspended load transport. *J Hydraul Eng,* Vol.110, No.11, pp. 1613–1614

van Rijn, L.C. (1984c). Sediment transport–part 3: bed forms and alluvial roughness. *J Hydraul Eng,* Vol.110, No.12, pp. 1733–1754

Vongvisessomjai, S.; Chowdhury, S.H. & Huq, M.A. (1983). *Monitoring of Shoreline and Seabed of Map Ta Phut Port*. Tech. Rep. 262, AIT Research Report, Bangkok, Thailand

Warren, I.R. & Bach, H.K. (1992). MIKE21: a modelling system for estuaries, coastal waters and seas. *Environmental Software*, Vol.7, pp. 229-240

Work, P.A.; Guan, J.; Hayter, E.J. & Elci, S. (2001). Mesoscale model for morphological change at tidal inlet. *Journal of Waterway Port Coastal and Ocean Engineering,* Vol.127, No.5, pp. 282-289

Xie, D.; Wang, Z.; Gao, S. & de Vriend, H. J. (2009). Modeling the tidal channel morphodynamics in a macro-tidal embayment, Hangzhou Bay, China. *Continental Shelf Research*, Vol.29, pp. 1757-1767

Zhang, Y.; Baptista, A.M. & Myers, E.P. (2004). A cross-scale model for 3D baroclinic circulation in estuary-plume-shelf systems: I. Formulation and skill assessment. *Cont Shelf Res*, Vol.110, No.10, pp. 1431–1456

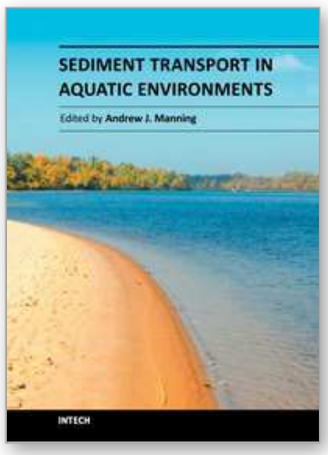

Sediment Transport in Aquatic Environments

Edited by Dr. Andrew Manning

ISBN 978-953-307-586-0

Hard cover, 332 pages

Publisher InTech

Published online 30, September, 2011

Published in print edition September, 2011

Sediment Transport in Aquatic Environments is a book which covers a wide range of topics. The effective management of many aquatic environments, requires a detailed understanding of sediment dynamics. This has both environmental and economic implications, especially where there is any anthropogenic involvement. Numerical models are often the tool used for predicting the transport and fate of sediment movement in these situations, as they can estimate the various spatial and temporal fluxes. However, the physical sedimentary processes can vary quite considerably depending upon whether the local sediments are fully cohesive, non-cohesive, or a mixture of both types. For this reason for more than half a century, scientists, engineers, hydrologists and mathematicians have all been continuing to conduct research into the many aspects which influence sediment transport. These issues range from processes such as erosion and deposition to how sediment process observations can be applied in sediment transport modeling frameworks. This book reports the findings from recent research in applied sediment transport which has been conducted in a wide range of aquatic environments. The research was carried out by researchers who specialize in the transport of sediments and related issues. I highly recommend this textbook to both scientists and engineers who deal with sediment transport issues.

InTech Europe
University Campus STeP Ri
Slavka Krautzeka 83/A
51000 Rijeka, Croatia
Phone: +385 (51) 770 447
Fax: +385 (51) 686 166
www.intechopen.com

InTech China
Unit 405, Office Block, Hotel Equatorial Shanghai
No.65, Yan An Road (West), Shanghai, 200040, China
中国上海市延安西路65号上海国际贵都大饭店办公楼405单元
Phone: +86-21-62489820
Fax: +86-21-62489821

IntechOpen